Earthquake Engineering and Structural Dynamics

Vol. 12, No. 6 *November–December 1984*

INTERNATIONAL JOURNAL FOR NUMERICAL METHODS IN ENGINEERING, VOL. 21, 389–407 (1985)

THE CURVED BEAM/DEEP ARCH/FINITE RING ELEMENT REVISITED

GANGAN PRATHAP†

Structural Sciences Division, National Aeronautical Laboratory, Bangalore, India

SUMMARY

In this paper, an attempt is made to understand the errors arising in curved finite elements which undergo both flexural and membrane deformations. It is shown that with elements of finite size (i.e. a practical level of discretization at which reasonably accurate results can be expected), there can be errors of a special nature that arise because the membrane strain fields are not consistently interpolated with terms from the two independent field functions that characterize such a problem. These lead to errors, described here as of the 'second kind' and a physical phenomenon called 'membrane locking'.

The findings here emerge from recent research on the effect of reduced integration on shallow curved beam elements and on the use of coupled displacement fields in finite rings. The failures which have occurred in earlier attempts to use independent polynomial displacement fields for curved elements may not have been due to neglect of rigid body motions or failure to achieve constant strain states, but because of locking due to spurious constraints. These emerge in the penalty limits of extreme thinness (an inextensional regime), when exact integration of the energy functionals of an element based on low order independent interpolations for the in-plane and normal displacements is used.

It seems possible to determine optimal integration rules that will allow the extensional deformation of a curved beam/deep arch/finite ring element to be modelled by independently chosen low order polynomial functions and which will recover the inextensional case in the penalty limit of extreme thinness without spurious locking constraints. The much maligned 'cubic in w–linear in u' curved beam element is now reworked to show its excellent behaviour in all situations. What is emphasized is that the choice of shape functions, or subsequent operations to determine the discretized functionals, must consistently model the physical requirements the problem imposes on the field variables. In this manner, we can restore an old element to respectability and thereby indicate clearly the underlying principles. These are: the importance of 'field consistency' so that arch and shell problems can be modelled consistently by independent polynomial displacement fields, and the role that reduced integration or some equivalent construction can play to achieve this.

INTRODUCTION

A large body of literature on the use of reduced integration and selective integration and other equivalent constructions (e.g. smoothed shape functions, discontinuous force mixed models, hybrid stress models, introduction of bubble modes to produce incompatible elements, independent shear strain interpolation, etc.) in shear flexible bending elements exists and continues to grow rapidly.[1–9] Recent evidence makes it clear now that the 'shear locking' that emerges at penalty function limits of extreme thinness (i.e. tending to Kirchhoff plate theory) arises due to inconsistencies in the number of constants required to define interpolations for θ_x and $w_{,x}$ and θ_y

†Presently at: Institut fur Strukturmechanik, DFVLR, 3300 Braunschweig, W. Germany.

0029–5981/85/03 0389–19$01.90

Received 9 February 1983
Revised 31 January 1984

and $w_{,y}$ (the rotations of the normals and the derivatives of the transverse displacements in each case) when equal order interpolations are used for w, θ_x and θ_y.[10,14] This problem can be alleviated in many ways; for example, by selectively integrating the shear energy terms[1-10] or by the use of rationally chosen stress functions in the hybrid stress approach[11-13] such that the spurious constraints that emerge in the thin plate limit when exact integration is used are selectively removed and only the true Kirchhoff constraints are retained.

The study of curved beam/deep arch/finite ring elements has generated considerable interest as it had direct bearing on the very serious difficulties encountered with more generally curved elements, e.g. shells. For many years, it has been thought that most of the difficulties that arose when low order independent interpolations were used for the normal and tangential displacements of singly curved and doubly curved elements were due to the fact that the usual low-order polynomial functions for tangential and normal displacements of the curved surface[15,16] do not admit unstressed rigid body motion of the arch/shell elements. In Reference 17, these simple functions were modified with the inclusion of trigonometric terms meant to improve the strain-free rigid-body displacement modes, and a dramatic improvement in results was found. The remarkable inaccuracy of the curved beam model using a linear polynomial for the tangential displacement u and a cubic polynomial for normal displacement w was therefore attributed to the inability of these low order independent polynomial functions to represent rigid body motions explicitly.[18,19]

The need for exact representation using transcendental terms of the strain-free rigid-body modes is still a matter of controversy, in view of the argument that trigonometric terms can be expanded in truncated power series form and that it should be possible to use finite polynomials provided the subtended angle formed by the element was small. Thus, quite early in the literature, observations had already been made that an explicit representation of the rigid-body modes need not be made,[20,21] provided that sufficiently high interpolation orders were made available to ensure that rigid-body modes can appear asymptotically.[22,23] It was thought that the poor performance of many curved elements was often due to the use of polynomial surface displacements of too low an order and that assumptions of polynomial surface displacements of sufficiently high order, e.g. the quintic–quintic element of Dawe,[24] would recover quite closely, the transcendental functions in the expression of rigid body modes. Moreover, the use of a high order polynomial surface displacement field in conjunction with conventional shell theory, also permits better representation of the solution of an important class of 'sensitive' problems. These are those problems where the low energy inextensional bending solutions occur and the variation of the normal displacement field of order m would be accompanied by a variation in tangential displacement in polynomial form of order $m+1$.

An attractive alternative to the use of high order independent polynomial representation was an analysis based on the assumption of constant axial strain and linear bending strain and integrating these to get a linear polynomial field in w and a quadratic polynomial field in u, which are coupled, and then combining these with simple trigonometric terms so that both constant strain and rigid-body conditions are met.[25-27] This proved to be a very efficient element.

Thus, when the state of the art on the subject was reviewed,[28] it was thought that the major difficulties encountered in arch and shell analysis were the requirements of constant strain rate, strain-free rigid-body displacement modes and the need to satisfy 'sensitive' solution requirements in low energy inextensional cases and that these can be met by the use of a high order independent interpolation field (quintic–quintic) or by the use of coupled polynomial displacement fields (linear w, quadratic u) together with trigonometric fields.

More recently, Meck[29] showed that failures which have occurred in earlier attempts to use only polynomial functions for curved elements were not due to the neglect of rigid-body motions, but due to the neglect of the coupling required between normal and tangential displacements for the inextensibility condition. He proposed a coupled displacement field for u and w such that the inextensibility condition is satisfied, and formulated an extensional model separately by addition of an extensional energy term in terms of a strain parameter (as a nodeless variable). Alternatively, for a generalised version of independent displacement function fields for these 'sensitive' problems, he suggested

$$u = a_1 + a_2\theta + \cdots + a_{m+1}\theta^m$$
$$v = b_1 + b_2\theta + \cdots + b_{n+1}\theta^n$$

where $m = n+1$ is to be satisfied to get good results. Thus, the familiar cubic in w element would require a quartic in u to ensure good results.

It was only recently that the role that reduced integration can play in evaluating the extensional energy of a curved beam was identified.[14,30,31] In Reference 14, Prathap and Bhashyam examined a shallow curved Timoshenko beam and showed that an exact integration of the extensional energy term created a mechanism that they called 'in-plane locking' that delayed convergence and that reduced integration of these terms improved the performance of the shallow curved beam. The work of Noor and Peters[30] observed that inextensional (or nearly inextensional) deformations are poorly represented by stiffness models based on exact integration of low order independent interpolations for displacement and rotational components unless a reduced integration of the displacement model or equivalently, a discontinuous force field mixed model is used. They attribute this to the inadequate representation of rigid-body modes and a magnification of the errors in the extensional energy term by a factor proportional to the ratio of the radius of curvature of the arch to its thickness. Very similar arguments had earlier formed the basis of the residual energy balancing methods of Fried.[32-34] However, it still remained unclear how reduced integration, which effectively smooths and therefore reduces the order of the polynomial displacement fields used to calculate the extensional energy, can improve the representation of the rigid-body modes if indeed this was the crux of the problem.

Independently of Prathap and Bhashyam,[14] Stolarski and Belytschko[31] observed that when low order in-plane displacement fields were used for a Marguerre-type shallow shell theory to model a curved beam, an exact integration caused an apparent increase in bending stiffness due to the curvature coupled membrane strains and that this can be alleviated by using reduced integration on the extensional energy terms. This action was called 'membrane locking', but no compelling explanation for the actual origin of locking or on how to determine the optimal order of integration of the extensional energy terms for a given pair of independent displacement fields was available.

In this paper, we try to unify the concepts that emerge from the work cited above and especially of that in References 14 and 29–31. It is seen that when low order interpolations are used for the inplane displacement terms, the inconsistency in the number of constants required to define interpolations for the $u_{,y}$ and w/R terms in the extensional strain energy functional produces spurious constraints in the penalty limit of extreme thinness (i.e. nearly inextensional behaviour) and these cause the locking of the solution. These errors of the second kind[14,19] can be removed by optimally integrating the extensional energy terms so that only the true constraints in the inextensional limit are retained. Thus the general extensional deformation behaviour of a curved beam can be modelled by independently chosen low order polynomial functions and this will still recover the inextensional case in the penalty limit without spurious constraints provided selective integration is used. In the next section, we re-work the 'cubic in w–linear in u' curved beam/arch/finite ring element (henceforth CL element) to show its excellent behaviour in all situations, after providing for optimal integration.

ANALYSIS OF THE 'CUBIC IN W–LINEAR IN U' ELEMENT

Element description

We start with the simplest shape function representation in the literature that ensures C_0 continuity for the tangential displacement u and C_1, continuity for the normal displacement w corresponding to the thin curved beam/deep arch/finite circular ring model (Figure 1):

$$u = b_1 + b_2 y$$
$$w = a_1 + a_2 y + a_3 y^2 + a_4 y^3 \tag{1}$$

One of its major virtues is that it has 3 degrees-of-freedom per node i.e. u, w and θ (the rotation), and is easily compatible with most general-purpose codes which allow the three basic displacements and three basic rotations. In comparison, the most successful element in the literature, the quintic–quintic requires 6 degrees-of-freedom per node. So there is considerable virtue in being able to restore this cubic–linear element to some degree of usefulness.

The extensional strain and change of curvature are

$$\varepsilon = u_{,y} + w/R$$
$$\chi = \frac{1}{R}u_{,y} - w_{,yy} \tag{2}$$

and the total energy of an element of length $2L$ is

$$U = \int_{-L}^{L} \left(\frac{EA}{2}\varepsilon^2 + \frac{EI}{2}\chi^2 \right) \mathrm{d}y \tag{3}$$

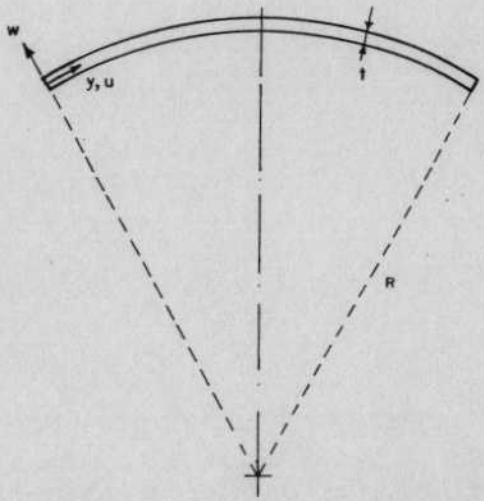

Figure 1. Geometry of a curved beam/circular arch/finite ring element

Discretization of the strain energy functional

Following Reference 14, we examine the terms arising from the discretized functional U above. We have

$$U = U_1 + U_2$$

where

$$U_1 = \frac{Ebt}{2}\int_{-L}^{L} \left(b_2 + \frac{a_1}{R} + \frac{a_2 y}{R} + \frac{a_3 y^2}{R} + \frac{a_4 y^3}{R} \right)^2 \mathrm{d}y \tag{4}$$
$$U_2 = \frac{Ebt^3}{24}\int_{-L}^{L} \left(\frac{b_2}{R} - 2a_3 - 6a_4 y \right)^2 \mathrm{d}y$$

After carrying out the discretization and regrouping of terms, we have

$$U_1 = \frac{Ebt}{2}\cdot 2L\left[\left(b_2 + \frac{a_1}{R} + \frac{a_3 L^2}{3R} \right)^2 + \frac{1}{3}\left(\frac{a_2 L}{R} \right)^2 \right.$$
$$\left. + \frac{4}{25}\left(\frac{a_3 L^2}{R} \right)^2 + \frac{2}{5}\left(\frac{a_2 L}{R} \right)\left(\frac{a_4 L^3}{R} \right) + \frac{1}{7}\left(\frac{a_4 L^3}{R} \right)^2 \right] \tag{5}$$
$$U_2 = \frac{Ebt}{24}\cdot 2L\left[\left(\frac{b_2}{R} - 2a_3 \right)^2 + 36\frac{a_4^2 L^2}{3} \right]$$

Constraints in inextensional limit

Comparing the energy terms, and following the arguments of Reference 14, we see that in the penalty limit of extreme thinness there are penalty terms that tend to enforce the following constraints:

$$b_2 + \frac{a_1}{R} + \frac{a_3 L^2}{3R} = 0$$
$$a_2 = 0 \tag{6}$$
$$a_3 = 0$$
$$a_4 = 0$$

The first constraint has terms from both interpolation functions and therefore enforces a valid constraint that implies the inextensibility condition

$$(u_{,y})_0 - \bar{w}/R = 0$$

where $\bar{w}$ is the normal deflection of some reference point on the element and the subscript 0 indicates the value at the mid-point of the element. This, therefore, is a simple measure of the averaged constant membrane strain in the element and, in the penalty limit, it is constrained to take a zero value.

On the other hand, $(a_2, a_3, a_4) \to 0$ imply that $(w_{,y})_0$, $(w_{,yy})_0$ and $(w_{,yyy})_0 \to 0$ are enforced in the penalty limit and are therefore spurious constraints. These lead to the locking phenomenon which we described as 'in-plane locking' in Reference 14, or as 'membrane locking' in Reference 29. It is quite simple to remove the locking terms by reduced integration. For the orders of the interpolation functions chosen above, a one-point Gaussian integration would give only the single

true inextensibility constraint,

$$b_2 + \frac{a_1}{R} = 0 \tag{7}$$

Any higher order integration rule will introduce the spurious constraints and an order that ensures exact integration will introduce all three spurious constraints. These spurious constraints are responsible for the errors of the second kind, as defined in Reference 14, and cause the severe deterioration of results with increasing penalty multiplier value, i.e. $(L/t)^2$. It is instructive to see how this emerges.

Functional reconstitution after discretization with finite size element

The method of functional reconstitution after discretization has been explained very clearly in Reference 14 to show how shear locking emerges in a simple linear shear flexible beam element in which the normal displacement w and face rotation θ are independently interpolated. We now adopt this approach to trace the origin of membrane locking to the use of independent interpolations for the two field variables here, u and w.

We consider the strain energy in an elemental arch of length $2L$ in a truly inextensional limit. We recognize that the extensional energy term due to the true constraint will vanish in this limit, but not the extensional energy contributions from the spurious terms. Thus for the discretized element of finite length $2L$, we observe that the strain energy density in an inextensional limit will be of the type (here, we consider only the two leading locking terms in U_1 as these will have the greater effect),

$$U = \frac{Ebt^3}{24}\left[\left(\frac{b_2}{R} - 2a_3\right)^2 + 36\frac{a_4^2 L^2}{3}\right] + \frac{Ebt}{2}\left[\frac{1}{3}\left(\frac{a_2 L}{R}\right)^2 + \frac{4}{45}\left(\frac{a_3 L^2}{R}\right)^2\right] \tag{8}$$

This has been obtained by dividing the strain energies of the element in equation (5) by its length. We observe, now, the presence of the L term in equation (8). In the real infinitesimal limit, the contributions to the extensional strain energy from the a_2, a_3 and a_4 terms will disappear, due to vanishing L without enforcing any constraints on these terms. However, in a real analysis, we need to work with a practical discretization (i.e. a finite L) and still expect reasonably accurate results to be obtained. This is the crux of the problem. With finite L, in the inextensional limit characterized by $t \gg t^3$ in equation (8), the membrane strain energy contribution is made to vanish by a_2 and a_3 tending to zero. These constraints are physically equivalent to an altered system in the non-penalty regime, which we can obtain by reconstituting a functional for the effective strain energy of an arch element based on a finite size discretization, as

$$\begin{aligned} U &= \frac{Ebt^3}{24}\int_{-L}^{L} w_{,yy}^2 \mathrm{d}y \\ &\quad + \frac{Ebt}{2}\int_{-L}^{L} \frac{1}{3}\left(\frac{L}{R}\right)^2 w_{,y}^2 + \frac{1}{45}\left(\frac{L^2}{R}\right)^2 w_{,yy}^2 \mathrm{d}y \\ &= \frac{EI}{3}\int_{-L}^{L}\left(1 + \frac{4}{15}\left(\frac{L^2}{Rt}\right)^2\right) w_{,yy}^2 \mathrm{d}y + \frac{1}{2}\cdot\frac{EAL^2}{3R^2}\int_{-L}^{L} w_{,y}^2 \mathrm{d}y \end{aligned} \tag{9}$$

Thus, when a finite size element of length L is used, the element after discretization of the

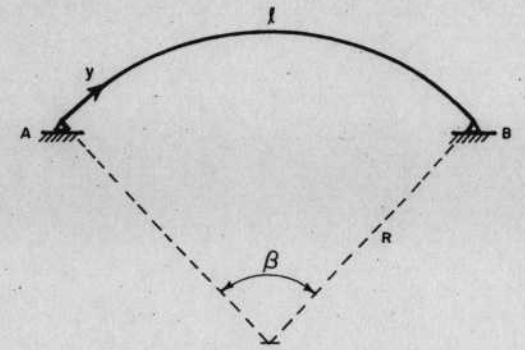

Figure 2. Shallow circular arch under uniformly distributed load

functionals, acts as a system with an altered modulus of inertia

$$I' = I\left(1 + \frac{4}{15}\left(\frac{L^2}{Rt}\right)^2\right)$$

and is further stiffened by a spurious in-plane force $F = EAL^2/3R^2$. It is necessary to recognize which of these two terms will play the leading stiffening role.

Consider the very simple example of a very shallow circular arch of length l and radius of curvature R (Figure 2), simply-supported at the ends and subtending an angle $\beta = 1/R$ at the centre. A uniformly distributed load is assumed to act on it and we may take a simple one term approximation for the normal deflection in the form,

$$w = c\sin\left(\frac{\pi y}{l}\right) \tag{10}$$

so that, when the entire arch is discretized by arch elements of length $2L$,

$$\begin{aligned} U &= \frac{1}{2}\int_0^l EI\left(1 + \frac{4}{15}\left(\frac{L^2}{Rt}\right)^2\right)\frac{c^2\pi^2}{l^4}\sin^2\left(\frac{\pi y}{l}\right)\mathrm{d}y \\ &\quad + \frac{1}{2}\int_0^l \frac{EAL^2}{3R^2}\frac{c^2\pi^2}{l^2}\cos^2\left(\frac{\pi y}{l}\right)\mathrm{d}y \end{aligned} \tag{11}$$

The total altered stiffness of the model can now be shown to be

$$\frac{\pi^4}{l^4}EI\left\{1 + \frac{4}{15}\left(\frac{L}{R}\right)^2\left(\frac{L}{t}\right)^2 + \frac{4}{\pi^2}\left(\frac{1}{R}\right)^2\left(\frac{L}{t}\right)^2\right\} \tag{12}$$

Since $l \gg L$ when a sufficiently large number of elements are used, the term from the in-plane stiffening force will be the principal stiffening factor and we can identify the principal locking term to depend on a structural parameter of the type $(\beta L/t)$ which will now act as the penalty multiplier term. Numerical experiments in the next section will establish that this is indeed true.

NUMERICAL EXPERIMENTS WITH THE CL ELEMENT

In the computer implementation of the CL element, provision was made to evaluate the stiffness matrix contributions from the bending energy and the membrane energy separately using

Gaussian integration orders that could be varied in each case. The order of the energy functionals dictate a 4-point integration rule for the exact evaluation of the membrane energy terms and a 2-point rule for the exact evaluation of the bending energy terms. Options for all rules from 1-point to 4-point were provided.

First, it was seen if with a 1-point integration of the membrane energy (a 4-point rule is adopted for the bending energy throughout), the CL1 element, could reproduce straight beam theory, as this was suggested by Gallagher[35] as a severe test for the strain element.[36] One half of a clamped–clamped beam under a central concentrated load (see Figure 3) with an l/t ratio of 125·6 and a R/t ratio of 2×10^8 was modelled with two CL1 elements. With $E = 1{\cdot}0$ and $F = 1{\cdot}0$, the result obtained, w(FEM) = 2477·0 compared very well with the elementary beam theory prediction of w(theory) = 2477·0. Thus, it is evident that with a 1-point integration of the membrane energy, no locking due to the errors of the second kind (i.e. errors induced by spurious constraining according to the terminology of Reference 14) had taken place even at such large values of L/t and R/t.

Next, one half of a clamped–clamped arch with a central concentrated load was studied, again with only two elements to model this half of the structure. A shallow and deep arch were defined to have a subtended angle $\beta = 1$ rad and $\pi/2$ rad, respectively (see Figure 4). A previous exercise has shown that in cases where the convergence of finite element results is delayed due to errors of the second kind, it is useful to define an additional stiffening factor e in terms of the finite element results w(FEM) and the theoretically predicted results w(theory) as

$$e = \frac{w(\text{theory})}{w(\text{FEM})} - 1 \tag{13}$$

This parameter would now be directly dependent on the structural parameter or parameters that

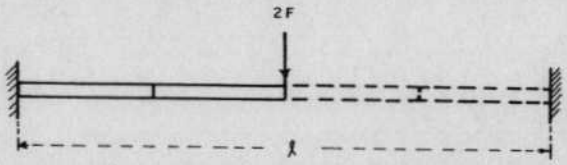

Figure 3. Clamped–clamped beam under a central concentrated load

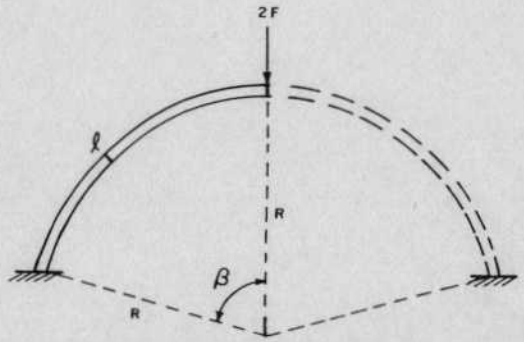

Figure 4. Clamped–clamped circular arch under central concentrated load

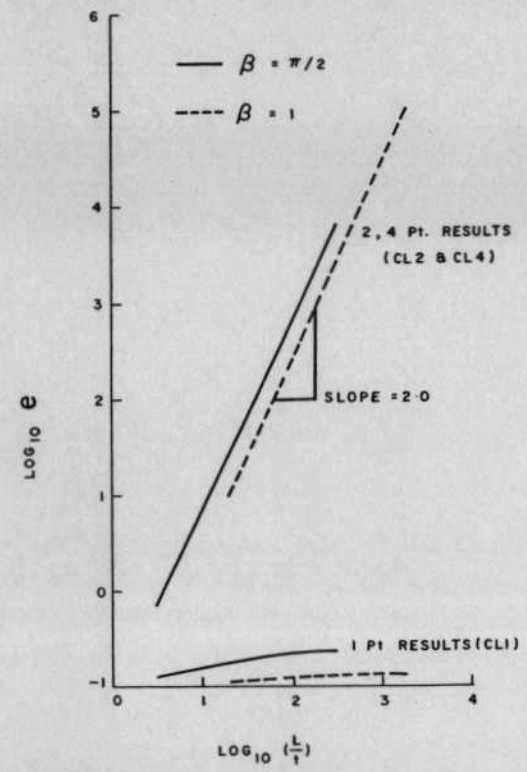

Figure 5. Additional stiffness parameter for clamped arch under central concentrated load

magnify the errors of the second kind in the penalty limits and therefore causes that phenomenon known as 'locking'.

Figure 5 shows the variation of Log e vs. Log (L/t) for the shallow and deep arches defined above. With a 1-point integration of the membrane energy (CL1), there was no rapid deterioration of the results with increase in the parameter L/t over a range 3·142 to 314·2 and 20·0 to 2000·0 in each case, and any errors present can be attributed to those described as errors of the first kind in the terminology introduced in Reference 14. However, with 2-point and 4-point integrations of the membrane energy (CL2, CL4), the locking is nearly identical and, in any case, too close to be separated on the Log–Log plot in Figure 5. The locking can be seen to very almost exactly as $(L/t)^2$, showing that errors of the second kind virtually dominate the behaviour in such limits. With increasing β, both the errors of the first and second kind increase. Our simple shallow circular arch example had predicted a structural multiplier term of the type $(\beta L/t)^2$. Thus a replot of the CL2 and CL4 results in the form Log e vs. Log $\beta L/t$ in Figure 6 yields a slope of 2·00 and does indicate a locking term of the kind $(\beta L/t)^2$ is indeed operative unless removed by a 1-point integration of the extensional energy.

Next, we examine the convergence of results with increase in the number of elements. We see that the CL1 element demonstrates an acceptable convergence rate typical of elements which have only

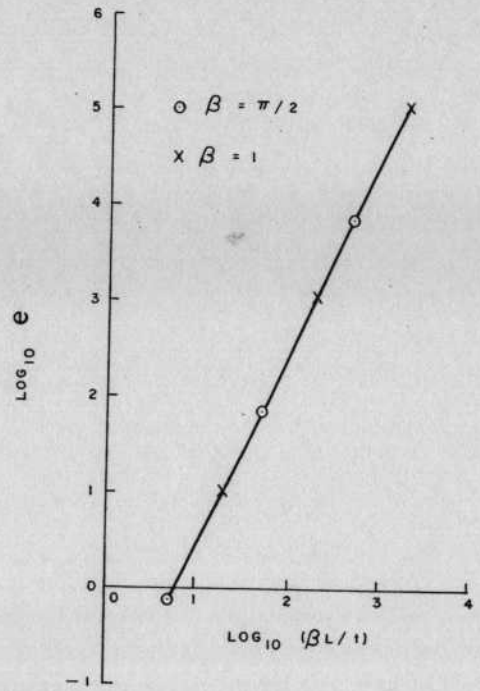

Figure 6. Additional stiffness parameter for clamped arch under central concentrated load

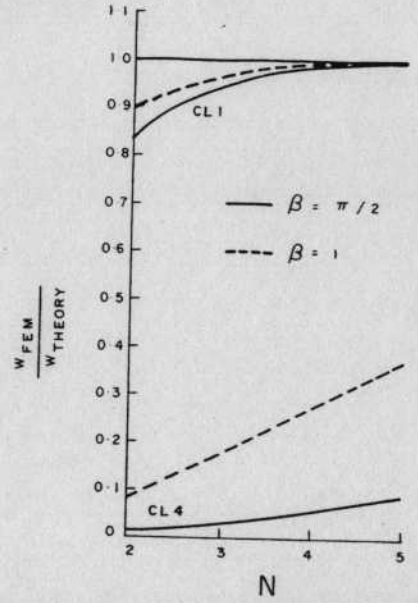

Figure 7. Convergence of deflection under central concentrated load on clamped arch with increase in number of elements

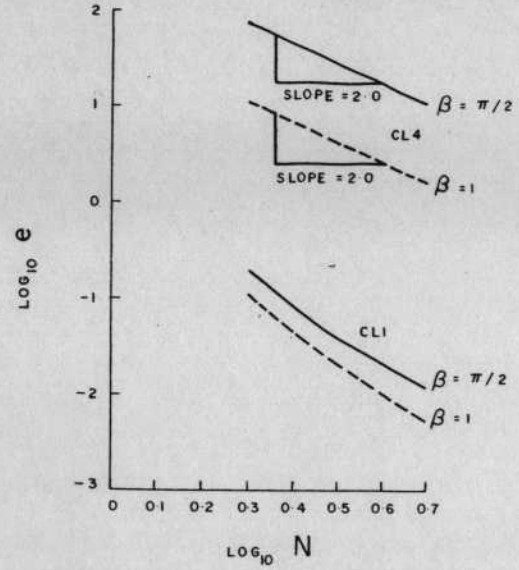

Figure 8. Convergence of additional stiffening parameter

errors of the first kind (Figure 7). However, the CL4 element converges, but in a much delayed rat typical of errors of the second kind. The R/t ratio for this case was 40. For an arch of fixed geometry (i.e. fixed β and R/t) idealized by N equal length elements, we expect from our error analysis in th earlier section that where errors of the second kind are present, the additional stiffening paramete e will vary as $1/N^2$. Figure 8 shows that this is indeed true in a typical case ($\beta = \pi/2$ and 1, $R/t = 40$

RE-EXAMINATION OF EARLIER WORK

It was observed by Meck[29] that a survey of the available results in the literature indicated tha improved displacement functions which included the transcendental terms for explicit rigid-body motions did give better results,[18,26,27] but that these also included some degree of coupling. It i more accurate to say, in the light of the evidence here, that what is necessary is that the polynomia interpolation for u should be complete and one order higher than that for w so that the 'sensitive solutions are covered and so that, in the inextensional limit, there would be a consistent field definition for the membrane strain which would not lead to errors of the second kind. Alternatively an optimum integration rule must be used to evaluate the membrane energy in the case o 'inconsistent' field definitions for u and w so that the contributions to membrane energy would b consistently represented by terms from both fields.

Low order elements

We can rework one of the earliest definitive results by Murray,[18] on the very poor performance of the CL element as compared even to a straight beam idealization of a circular arch. Element B1 i the same CL4 element considered in this paper and element B2 is a transformed CL element. Since

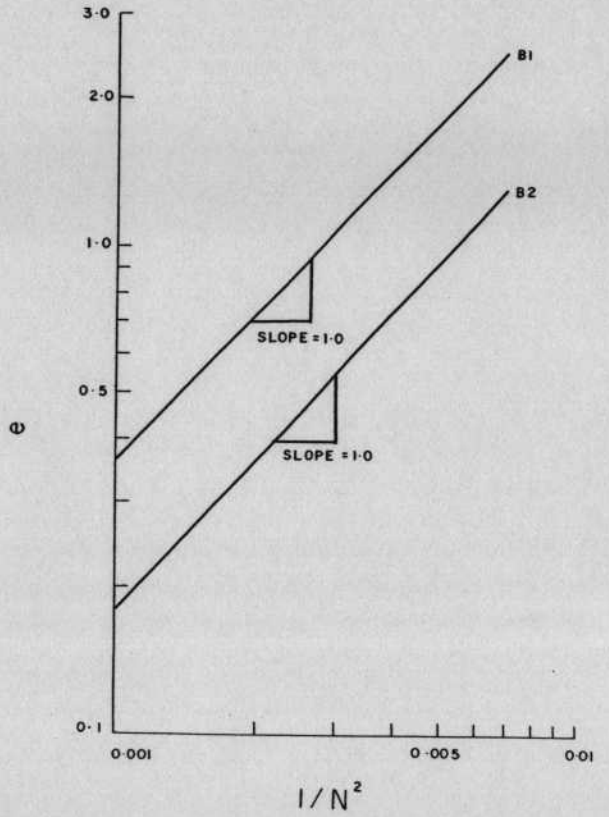

Figure 9. Additional stiffening parameter for a circular archproblem (Murray[18])

for B1, we would expect that, at least in a shallow thin case, the additional stiffness parameter due to errors of the second kind would vary as $(\beta L/t)^2$, for a given circular arch idealized by N elements, we would expect that this locking parameter would vary linearly with $1/N^2$. Figure 9 shows a plot of e vs. $1/N^2$ (these are projected from graphical results of Murray[18]). Since the values of e are so large even at such large values of N (errors of 50 per cent and above for N in the range 12 to 20), these are errors of the second kind. It is seen from Figure 9 that these errors of the second kind vary almost exactly in the $1/N^2$ fashion. Element B2 is also seen to lock in the same $1/N^2$ manner, showing again that the transformation meant to remove the constrained rigid-body modes was not sufficient to obviate membrane locking, as it could not ensure a consistent definition of strain in terms of constants from the linear and cubic polynomials used.

We can also rework the basic findings reported by Ashwell in Chapter 6 of Reference 28 as follows. We note that the Gallagher[15] and Connor–Brebbia[16] shape functions, when adapted for an arch, become the familiar cubic–linear element we have used here,

$$u = b_1 + b_2 y$$
$$w = a_1 + a_2 y + a_3 y^2 + a_4 y^3 \qquad \text{(A)}$$

and both the Cantin–Clough[17] and Sabir–Lock[38] elements can be written in the form ($\phi = y/R$),

$$u = c_1 \cos\phi - c_2 \sin\phi + c_3 \cos\beta \cos\phi + b_1 + b_2 y$$
$$w = c_1 \sin\phi + c_2 \cos\phi + c_3 \cos\beta \sin\phi + a_3 y^2 + a_4 y^3 \qquad \text{(B)}$$

These constitute equations (A) and (B) of Chapter 6 of Reference 28. We shall study equations (B) in a similar manner as done for equations (A) in the earlier section. The membrane strain now becomes

$$\varepsilon = u_{,y} + w/R = b_1 + \frac{a_3 y^2}{R} + \frac{a_4 y^3}{R} \qquad (14)$$

Note that these terms are now inconsistent; the constant part of the membrane field has a parameter only from the polynomial for u, the linear part is missing and the quadratic and cubic terms have parameters only from the polynomial for w. Locking is to be expected, but the omission of the linear term in w would suggest that locking due to the a_2 term which existed in the CL4 element would be absent. Thus, the Cantin–Clough element should be marginally superior to the CL4 element. The discretized membrane energy for an element of length $2L$ would be

$$U_1 = \frac{Ebt}{2} \cdot 2L \left[\left(b_2 + \frac{a_3 L^2}{3R} \right)^2 + \frac{4}{45} \left(\frac{a_3 L^2}{R} \right)^2 + \frac{1}{7} \left(\frac{a_4 L^3}{R} \right)^2 \right] \qquad (15)$$

The first term, $(b_2 + a_3 L^2/3R)$ can produce a consistent constraint in the inextensional limit as it has terms from both field definitions (i.e. for u and w), but the terms $(a_3 L^2/R)$ and $(a_4 L^3/R)$ would be the inconsistent terms. Thus, although rigid-body modes have been explicitly included in the Cantin–Clough element, these would lock while enforcing the spurious constraints and this explains the progressive deterioration of the Cantin–Clough arch element as one proceeds through the series of thick–moderate, thin–moderate, thick–deep and thin–deep arches used as examples in Chapter 6 of Reference 28. Also, as locking originates principally from the $(a_3 L^2/R)$ terms, we can show in an analysis for a very shallow inextensional circular arch, as done earlier for the CL element, that for a fixed geometry (l, R, t fixed) idealized by N elements, the errors of the second kind would vary in a N^{-4} fashion as opposed to the CL element, where due to the locking originating with the $(a_2 L/R)$ term, it would vary in a N^{-2} fashion. We shall see later that this can be demonstrated. Thus, the improvement observed in the Cantin–Clough element was not due to the explicit inclusion of the rigid-body motion terms, but due to delaying the order at which the field definitions or shape-function contributions to the membrane energy become inconsistent.

The assumed strain element in the Chapter 6 of Reference 28 is based on the coupled interpolations

$$u = -c_1 \sin\phi + c_2 \cos\phi + b_1 + b_2 y + \frac{b_3}{2} y^2 \qquad (16)$$

$$w = c_1 \cos\phi + c_2 \sin\phi + a_1 - b_3 R y$$

so that the membrane strain becomes

$$\varepsilon = b_2 + a_1/R \qquad (17)$$

The membrane strain is now consistently represented with independent terms from both the u and w field interpolations and will yield the true inextensional constraint in the limit. Thus, it is not surprising that the convergence of this element is not dependent on arch type (i.e. the parameters l, R and t) or, in other words, there are no errors of the second kind. For further reference, this element would be called the SC element.

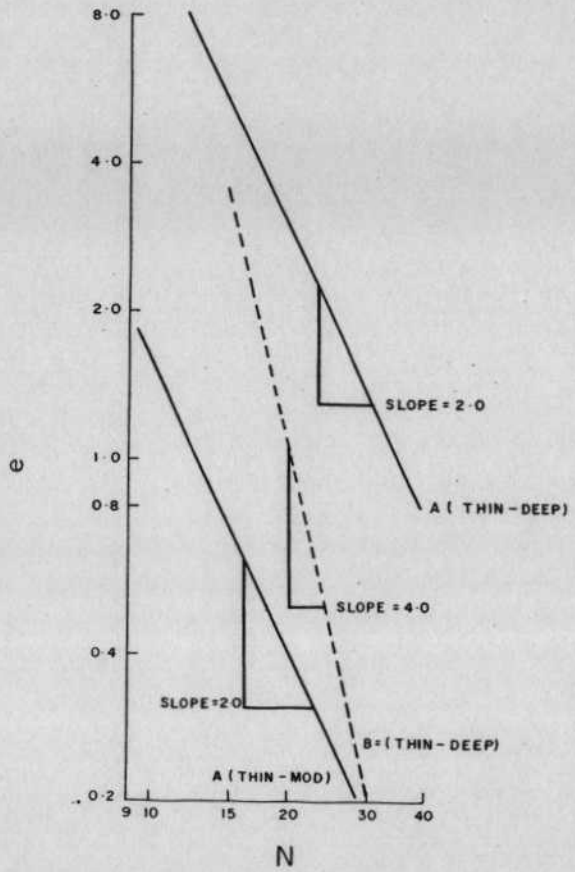

Figure 10. Additional stiffness parameter for a circular arch problem (Ashwell, Chapter 6 of Reference 28)

Figure 10 shows a reinterpretation of the results from Ashwell (Chapter 6 of Reference 28) for a thin–moderate and thick–deep arch for element A (based on equations (A) above) and a thin-deep arch for element B (based on equations (B) above). The additional stiffness factor e is plotted against the number of elements N for a centrally loaded encastre configuration. The slopes of the lines indicate very clearly that for element A, which is identical to CL4, the errors of the second kind do indeed vary in a N^{-2} fashion and that for element B, the errors of the second kind vary in a N^{-4} fashion, as established in this section. In contrast, the e values of the SC element are too small to be presented on this graph.

In order to study the dependence on arch type for element A, we plot the additional stiffness factors for a thin–moderate and thick–deep element on a single graph. In Figure 11, each point corresponds to the value of e obtained from the same N for the thin–moderate and thick–deep arches, respectively. The error model for element A suggests that the errors will be in the ratio $[(\beta^2 R/t)_2^2/(\beta^2 R/t)_1^2]$. The computed value for the arch geometries used by Ashwell is 6·41 and this agrees quite well with the slope from Figure 11, which is 6·43.

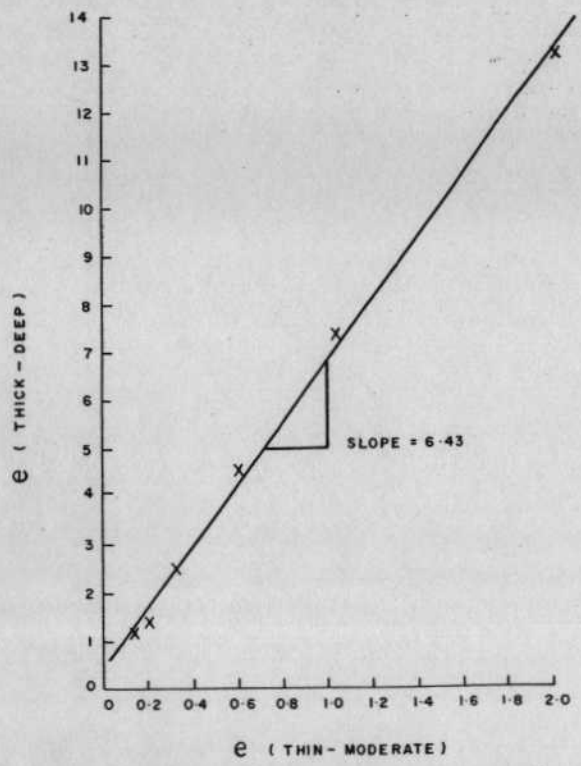

Figure 11. Comparison of errors of the second kind for two different arch geometries

High order elements

The first systematic study on the use of high order independent polynomial interpolations for u and w is summarized by Dawe in Chapter 8 of Reference 28. We shall rework the examples in that chapter as follows:

Quintic–quintic element:

$$u = b_1 + b_2 y + b_3 y^2 + b_4 y^3 + b_5 y^4 + b_6 y^5$$
$$w = a_1 + a_2 y + a_3 y^2 + a_4 y^3 + a_5 y^4 + a_6 y^5 \tag{18}$$

Now, the only inconsistent term in the membrane energy would be due to the $a_6 y^5$ term. This is an error of such low order that it would have very little influence even as errors of the second kind (perhaps of N^{-10} order) and this explains the remarkable accuracy of this element.

Cubic–quintic element:

$$u = b_1 + b_2 y + b_3 y^2 + b_4 y^3 + b_5 y^4 + b_6 y^5$$
$$w = a_1 + a_2 y + a_3 y^2 + a_4 y^3 \tag{19}$$

Again, there is one inconsistent term, but it is of the b_6y^5 type. Since it originates from the polynomial for u, a locking due to this term in the inextensional limit is not undesirable as it would only be enforcing the requirement that $u \to 0$ in comparison with the transverse deflection w. Thus, there would not be an error of the second kind in this element.

Cubic–cubic element:

$$u = b_1 + b_2y + b_3y^2 + b_4y^3$$
$$w = a_1 + a_2y + a_3y^2 + a_4y^3 \tag{20}$$

Now, locking is determined solely by the a_4y^3 term and, for the demonstration example of an inextensional shallow arch, this should depend on a structural parameter of the form $(\beta 1/N^3t)^2$.

Quintic–cubic element:

$$u = b_1 + b_2y + b_3y^2 + b_4y^3$$
$$w = a_1 + a_2y + a_3y^2 + a_4y^3 + a_5y^4 + a_6y^5 \tag{21}$$

Now, locking starts with the a_4y^3 term and also includes the a_5y^4 and a_6y^5 terms. The a_4y^3 term should dominate and this element should behave as badly as the CC element above. Indeed, Dawe observes that the QC element is less efficient than the CC element and that, in general, the efficiency of a curved element is not improved by increasing the order of the interpolation for the normal displacement without correspondingly increasing the order of the interpolation for the tangential displacement.

We can now re-examine some of the results presented by Dawe in Chapter 8 of Reference 28. Figure 12 shows a logarithmic plot of e vs. N for the CC case and the SC and CQ cases for the deep–thin, shallow–thin and deep–thick cases considered by Dawe. The shallow–thick case is not included here as it is evident from Dawe's results that, in this case, the relevant geometrical parameter is so low that it contributes little to errors of the second kind.

Our observations earlier in this section have indicated that the CC element should lock and that the CQ and SC elements should not. The geometrical parameter that should influence locking in the CC case can be written as $\beta L/N^3t$ or β^2R/N^3t or l^2/RtN^3, where β is the angle subtended by the half of the arch that is modelled ($\pi/2$ or $\pi/12$ for the deep and shallow cases, respectively), R is the radius of curvature and l is the total length of arch modelled by N elements of length L. Thus, if errors of the second kind are indeed present, then on an element basis the results should deteriorate with increase in β^2R/t in the CC idealization and should not be affected in the CQ and SC idealizations. For the three cases considered in Figure 12, the values of β^2R/t are 671, 72 and 41·9 and the dependence on geometry of the additional stiffness parameter e due to locking is obvious for the CC idealization. Also, the slope of the CC results for the shallow–thin case show very nearly a N^{-6} dependence, as is predicted from the $(l^2/RtN^3)^2$ factor. In contrast, for all three arch geometries, the SC and CQ models give identical accuracy on an element basis even for the large change in geometrical parameters from 41·9 to 671. So no errors of the second kind are present, as has been anticipated earlier. It appears that whatever errors that remain in the SC and CQ elements are errors of the first kind and are simple functions of the number of elements N used in the idealization. The QC results (not replotted here) behave almost in the same manner as the CC results, thus demonstrating that locking is initiated at the same order of inconsistency, namely with the a_4y^3 term.

A consideration of the moment and force distributions show that the SC and CQ models give smooth moment and force predictions over the arch and within elements. However, the CC and QC models give discontinuous moments and forces at nodes and rapid fluctuations within the element. Even the QQ model, which is remarkable for its accuracy in the prediction of deflections, shows considerable fluctuations for the force distribution. These observations further reinforce the

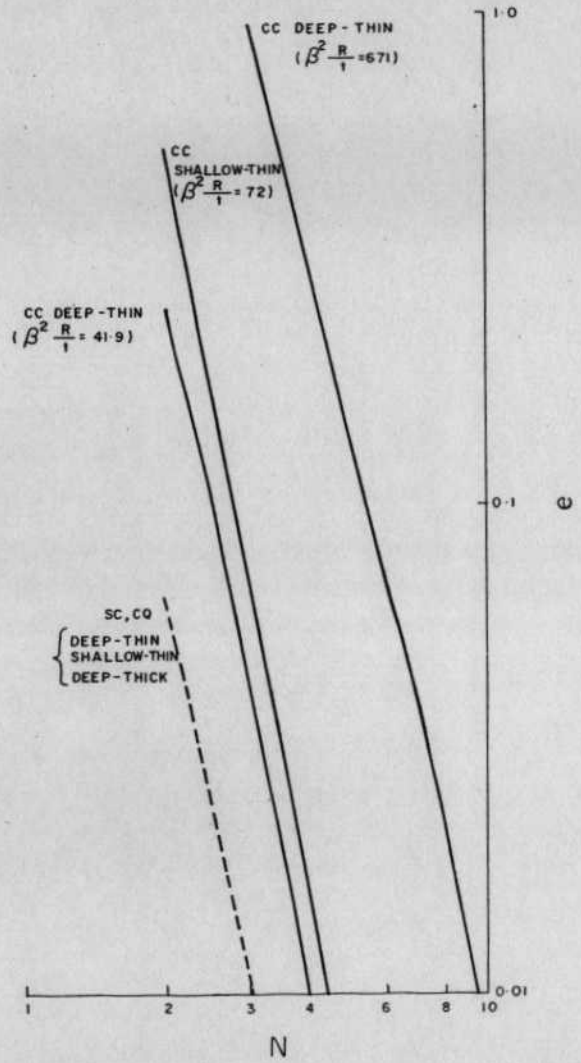

Figure 12. Additional stiffness parameter for a circular archproblem (Dawe, Chapter 8 of Reference 28)

importance of field consistency in evaluating membrane strains. It is also clear that, for the CL1 element, the best prediction for force and moment would be obtained at the point of integration for the membrane energy, i.e. the mid-point of the element.

CONCLUSIONS

The fact that overall reduced integration for both the shear and the membrane energy in thick and thin shell applications had a dramatic effect on accuracy and economy of use of the element was

established as early as in 1971 (References 1 and 2). However, it had little impact on subsequent thin shell and arch research where membrane locking plays an additional critical role, but considerable impact on straight beam and flat plate research where shear locking alone is critical. This must have been because the principles of shear locking were fairly well established by then, but the idea that membrane locking was due to the inconsistency of field definitions for the tangential and normal displacement contributions to the membrane strain was not made until fairly recently.[14,31] Thus, two recent innovations on shell elements,[4,8] have been very useful and efficient because they use correctly the selective integration rules required for membrane and shear energy, and while they emphasize the removal of shear locking with considerable mathematical rigour, they do not indicate how the improvement due to overall reduced integration can come about, in terms of the removal of spurious in-plane constraints.

In this paper, it has been possible to indicate general principles governing the errors of the second kind associated with the use of low order independent polynomial fields for thin arch and thin shell structures, and show how the in-plane constraints that arise in the very thin (inextensional) limit can be removed by an optimal application of integration rules. An old, familiar but till now discarded element has been reworked and shown to be useful, and should be a powerful candidate for inclusion in general-purpose libraries which deal with elements with few degrees-of-freedom per node. A shear flexible version of this element would indeed be that used by Noor and Peters[30] and will have linear interpolations for u, w and the face rotations θ and will have a one-point integration rule for the membrane and shear energies. It is clear that the unexpected accuracy of such simple elements in Reference 30 is due to the removal of spurious membrane constraints, in addition to the removal of spurious shear constraints.

A re-examination of earlier work in the light of the present observations shows that a treatment in terms of errors of the second kind accounts largely for the very poor behaviour of most elements which have used low order independent interpolations, and also explains why some of the coupled displacement fields which inherently establish consistent interpolation functions for u and w have been without errors of the second kind. Thus, a treatment in terms of the need for strain-free rigid-body modes is unnecessary, as, if this requirement were indeed necessary, then an application of reduced integration, which actually reduces the order of interpolation for the w contributions to the membrane energy, should have even more disastrous consequences. However, the early anticipation[39,40] for the need to satisfy 'sensitive' solutions by having interpolations for the tangential displacement of one order higher than that required for normal displacement is found to be substantially correct.

ACKNOWLEDGEMENTS

The author is very grateful to Mr. B. R. Somashekar, Head, Structures Division, for his constant support and encouragement. The author is also very thankful to the DAAD and to Dr. Ing. H. W. Bergmann, Director of the DFVLR Institute of Structural Mechanics at Braunschweig for the opportunity to work there on a DAAD Exchange Fellowship. He is also indebted to Mr. Ashok Kamath for help at all stages of the computational work.

REFERENCES

1. O. C. Zienkiewicz, R. L. Taylor and J. M. Too, 'Reduced integration technique in general analysis of plates and shells', *Int. j. numer. methods eng.*, **3**, 275–290 (1971).
2. S. F. Pawsey and R. W. Clough, 'Improved numerical integration of thick shell finite elements', *Int. j. numer. methods eng.*, **3**, 575–586 (1971).

3. T. J. R. Hughes, R. L. Taylor and W. Kanoknukulchai, 'A simple and efficient finite element for plate bending', *Int. j. numer. methods eng.*, **11**, 1529–1543 (1977).
4. R. H. Macneal, 'A simple quadrilateral shell element', *Comp. Struct.*, **8**, 175–183 (1978).
5. E. D. L. Pugh, E. Hinton and O. C. Zienkiewicz, 'A study of quadrilateral plate bending elements with reduced integration', *Int. j. numer. methods eng.*, **12**, 1059–1079 (1978).
6. T. J. R. Hughes, M. Cohen and M. Haroun, 'Reduced and selective integration techniques in the finite element method', *Nucl. Eng. Design*, **46**, 206–222 (1978).
7. T. J. R. Hughes and M. Cohen, 'The heterosis finite elements for plate bending', *Comp. Struct.*, **9**, 445–450 (1979).
8. H. Parisch, 'A critical survey of the nine node degenerated shell element with special emphasis on thin shell application and reduced integration', *Comp. Meth. Appl. Mech. Eng.*, **20**, 323–350 (1979).
9. T. J. R. Hughes and T. E. Tezduyar, 'Finite elements based upon Mindlin plate theory with particular reference to the four node bilinear isoparametric element', *J. Appl. Mech.*, **48**, 587–596 (1981).
10. G. Prathap and S. Viswanath, 'An optimally integrated 4-node quadrilateral plate bending element', *Int. j. numer. methods eng.*, **19**, 831–840 (1983).
11. R. L. Spilker and N. I. Munir, 'The hybrid stress model for thin plates', *Int. j. numer. methods eng.*, **15**, 1239–1260 (1980).
12. R. L. Spilker and N. I. Munir, 'A hybrid stress quadratic displacement mindlin plate bending element', *Comp. Struct.*, **12**, 11–21 (1980).
13. R. L. Spliker and N. I. Munir, 'A serendipity cubic displacement element for thin and moderately thick plates', *Int. j. numer. methods eng.*, **15**, 1261–1278 (1980).
14. G. Prathap and G. R. Bhashyam, 'Reduced integration and the shear flexible beam element', *Int. j. numer. methods eng.*, **18**, 195–210 (1982).
15. R. H. Gallagher, 'The development and evaluation of matrix methods for thin shell structural analysis', *Ph.D. thesis*, State Univ. of New York, Buffalo, New York (1966).
16. J. Connor and C. Brebbia, 'A stiffness matrix for a shallow rectangular shell element', *J. Eng. Mech. Div. ASCE*, **93**(EM5), 43–66 (1967).
17. G. Cantin and R. W. Clough, 'A curved cylindrical shell finite element', *A.I.A.A. J.*, **6**, 1057–1062 (1968).
18. K. H. Murray, 'Comments on the convergence of finite element solutions', *A.I.A.A. J.*, **4**, 815–816 (1966).
19. J. E. Walz, R. E. Fulton, N. J. Cyrus and R. T. Eppink, 'Accuracy of finite element approximations to structural problems', *NASA TN-D 5728* (1980).
20. J. A. Stricklin, D. R. Navaratna and T. H. H. Pian, 'Improvements on the analysis of shells of resolution by the matrix displacement method', *A.I.A.A. J.*, **4**, 2069–2071 (1966).
21. W. E. Haisler and J. A. Stricklin, 'Rigid-body displacement of curved elements in the analysis of shells by the matrix displacement method', *A.I.A.A. J.*, **5**, 1525–1527 (1967).
22. P. M. Mebane and J. A. Stricklin, 'Implicit rigid-body motion in curved finite elements', *A.I.A.A. J.*, **9**, 344–345 (1971).
23. F. K. Bogner, R. L. Fox and L. A. Schmit, 'A cylindrical shell discrete element', *A.I.A.A. J.*, **5**, 745–750 (1967).
24. D. J. Dawe, 'Some higher order elements for arches and shells', in *Thin Shells and Curved Members* (eds. D. G. Ashwell and R. H. Gallagher), Chapter 8, Wiley, London, 1976, pp. 131–153.
25. D. J. Dawe, 'A finite deflection analysis of shallow arches by the discrete element method', *Int. j. numer. methods eng.*, **3**, 529–552 (1971).
26. D. G. Ashwell and A. B. Sabir, 'Limitations of certain curved finite elements when applied to arches', *Int. J. Mech. Sci.*, **13**, 133–139 (1971).
27. D. G. Ashwell, A. B. Sabir and T. M. Roberts, 'Further studies in the application of curved finite elements to circular arches', *Int. J. Mech. Sci.*, **13**, 507–517 (1971).
28. D. G. Ashwell and R. H. Gallagher, Eds., *Finite elements for Thin Shells and Curved Members*, Wiley, London, 1976.
29. H. R. Meck, 'An accurate polynomial displacement function for finite ring elements', *Comp. Struct.*, **11**, 265–269 (1980).
30. A. K. Noor and J. M. Peters, 'Mixed models and reduced/selective integration displacement models for non-linear analysis of curved beams', *Int. j. numer. methods eng.*, **17**, 615–631 (1981).
31. H. Stolarski and T. Belytschko, 'Membrane locking and reduced integration for curved elements', *J. Appl. Mech.*, **49**, 172–178 (1971).
32. I. Fried, 'Basic computational problems in the finite element analysis of shells', *Int. J. Solids Struct.*, **7**, 1705–1715 (1971).
33. I. Fried, 'Shape functions and the accuracy of arch finite elements', *A.I.A.A.J.*, **11**, 287–291 (1973).
34. I. Fried, 'Finite element analysis of thin elastic shells with residual energy balancing and the role of the rigid body modes', *J. Appl. Mech.*, **42**, 99–104 (1975).
35. R. H. Gallagher, Review No. 6155, *App. Mech. Rev.*, **25**, 924 (1972).
36. D. G. Ashwell, 'The behaviour with diminishing curvature of strain-based arch finite elements', *J. Sound Vib.*, **28**, 133–137 (1973).
37. S. Viswanath and G. Prathap, 'A note on locking in a shear flexible triangular plate bending element', *Int. j. numer. methods eng.*, (to appear).
38. A. B. Sabir and A. C. Lock, 'A curved cylindrical shell finite element', *Int. J. Mech. Sci.*, **14**, 125–135 (1972).
39. L. S. D. Morley, 'Polynomial stress states in first approximation theory of circular cylindrical shells', *Q. J. Mech. Appl. Meth.*, **25**, 13–43 (1972).
40. A. J. Morris, 'A deficiency in current finite elements for thin applications', *Int. J. Solids Struct.*, **9**, 331–346 (1973).